# Color Image Segmentation Accomplished by an Adaptive Similarity Measure

Rodolfo Alvarado-Cervantes, Edgardo Felipe-Riveron

Center for Computing Research, National Polytechnic Institute, Mexico Juan de Dios Batiz w/n, Col Nueva Industrial Vallejo, P.O. 07738, Mexico ateramex@gmail.com; edgardo@cic.ipn.mx

Abstract. An interactive and semiautomatic image segmentation method is presented which, unlike most of the existing methods in the published literature, uses the color information of each pixel as a unit, thus avoiding color information scattering. The color information of every pixel is integrated by an adaptive color similarity function designed for direct color comparisons. At present, the vast majority of segmentation techniques are just monochromatic methods applied to the individual color components in different color spaces, and in different ways to produce a color composite. Our color integrating technique is direct, simple, and computationally inexpensive. The improvement in quality of our proposed segmentation technique and its quick result is significant with respect to other solutions

Keywords: Color image segmentation; Adaptive similarity function; HSI parameter distances.

## 1. Introduction

Image segmentation consists of partitioning an entire image into different regions, which are similar in some predefined manner. Segmentation is an important feature of human visual perception, which manifests itself spontaneously and naturally. It is also the most important and difficult task in image analysis and processing [1] [2] [3] [4] [6] [7]; all subsequent steps like characteristics extraction and recognition greatly depend on the quality of segmentation. Without a good segmentation algorithm, objects of interest in a complex image are difficult (often impossible) to recognize using automated techniques [1] [2] [3] [5] [6] [7] [12]. Therefore, considerable effort often is required in the design of algorithms that improve the probability of successful segmentation. At present, several segmentation techniques are available for color images, but most of them are just monochromatic methods applied on the individual planes in different color spaces where the results are combined later in different ways [10]. Their common problem is that when the color components of a particular pixel are processed separately the color information is so scattered in its components that most of the color perception is lost [6] [7] [10] [12].

© G. Sidorov, B. Cruz, M. Martínez, S. Torres. (Eds.) Advances in Computer Science and Engineering. Research in Computing Science 34, 2008, pp. 103-115 Received 31/03/08 Accepted 26/04/08 Final version 03/05/08

# 2. Previous Works

In past years, there has been a considerable amount of research dedicated to the problem of color image segmentation due to its importance and potential. It has taken a great attention because color is an effective and robust visual cue for characterizing an object from others. The current available techniques and approaches vary widely from extensions of classical monochromatic techniques [11] to mathematical morphology [6], wavelets [17] and quaternions [22], among others. Until very recently, the majority of the published approaches were simply monochromatic techniques applied to each color component image in different color spaces [10] [12].

Some color similarity measures and distances are presented in [2]. All these measures compare color pixels as units. They are all based in three dimensional vector representations of color in which each vector component corresponds to the RGB color channels.

In [6] a technique that combines geometrical and color features for segmentation extending concepts of mathematical morphology (for gray images) is presented to process color images. The final segmentation is obtained by fusing a region hierarchical partition image and a fine details image. In [7] the authors argue that the common polar color spaces such as HLS, HSV, HSI, etc. are unsuited to image processing and analysis tasks. After presenting three prerequisites for 3D-polar coordinate color spaces well-suited to image processing, they derive a coordinate representation which satisfies their prerequisites that they called Improved HLS (IHLS) space.

In [8] the suitability of 3D polar representation for quantitative image processing tasks is investigated. After a critical analysis of the gamma correction, a polar representation using the L1 norm is proposed. The authors validate the relevance of their own representation by means of luminance/saturation histograms, which exhibit observable alignments and therefore some kind of order. In [11] and [12] the authors present a segmentation method based on a series of linear combinations of the RGB color components and the equalization version of each of them to create 16 monochromatic images which are later combined to obtain the final partition. This segmentation method is the basis for works presented in [13] [15] and [16].

In the technique presented in [22] the color information for every pixel is represented and analyzed as a unit in the form of quaternions for which every component of the RGB color pixel corresponds to the i, j and k bases accordingly. This representation of color is shown to be effective in the context of segmenting color images into regions of similar color texture.

# 3. Description of the Method

The segmentation method proposed basically relies on the calculation of a color similarity function for every pixel in a RGB 24-bit true color image. Firstly, we compute the color centroid and color standard deviation of a small sample of few pixels that represents the desired color to be segmented using the technique we designed for that purpose.

The color similarity function uses the color standard deviation calculated from the pixel sample to adapt the level of color scattering in the comparisons. The result of a particular similarity function calculation for every pixel and the color centroid (meaning the similarity measure between the pixel and the representative color) generates what we call a Color Similarity Image (CSI), which is just a gray level image. Once obtained, a CSI can be processed with any tool of mathematical morphology used for gray level images, integrating color and geometrical information in this way. In those cases where color is a discriminating characteristic of objects of interest in a source image, only thresholding the CSI is necessary to complete the segmentation.

The proposed technique can be conceptually divided in two steps:

- 1. The generation of Color Similarity Images (CSI) from the input color image by solving Eq. (1) (shown below) for each pixel and the color centroid, meaning the similarity measure between each pixel and the object color to be segmented. Only color information is used in this step resulting as a pixel-oriented technique.
- 2. The application (if necessary) of any desired morphology technique for gray level images on the previously generated CSI. In this way geometric discriminating characteristics are introduced in the segmentation process.

By calculation our color similarity function, the color information of every pixel is processed as a whole without separating its color components.

To generate a CSI we need:

- 1. A color image in RGB 24-bit true color format.
- 2. A small set of pixels forming a sample of the color desired to be segmented.

From this sample of pixels we calculate the statistical indicators according to our HSI modified color model (see Section 3.5). This information is necessary to adapt the color similarity function in order to obtain the best results. Then, to obtain a CSI we calculate for every pixel (i,j) in the image the color similarity function S:

$$S_{i,i} = e^{\left(\frac{-a_1 \Delta_{h}^{2}}{2\sigma_{h}^{2}}\right)} e^{\left(\frac{-a_2 \Delta_{s}^{2}}{2\sigma_{s}^{2}}\right)} e^{\left(\frac{-a_3 \Delta_{i}^{2}}{2\sigma_{i}^{2}}\right)} e^{\left(\frac{-a_3 \Delta_{i}^{2}}{2\sigma_{i}^{2}}\right)}. \tag{1}$$

Where

$$e = 2.7182...$$

 $\Delta_h = \text{hue\_distance\_}\Delta_h (\text{hue}(i,j), \text{average\_hue})$ 

 $\Delta_s$  = saturation\_distance\_ $\Delta_s$  (saturation(i,j), average\_saturation)

 $\Delta_i$  = intensity distance  $\Delta_i$  (intensity (i,j), average intensity)

 $\sigma_h$  = Hue standard deviation of the sample

 $\sigma_s$  = Saturation standard deviation of the sample

 $\sigma_i$  = Intensity standard deviation of the sample

 $[a_1 \ a_2 \ a_3] = \text{Mask of refinement}; a_i \text{ can be either } 0 \text{ or } 1.$ 

Two modifications on standard HSI color space were necessary in order to create a consistent model to represent colors and color centroids:

1. Representation of hue. Instead of standard representation of hue as an angle in the range [0°-360°], hue is represented here as a normalized vector in R<sup>2</sup> (with magnitude 1 or 0). This representation has at least three advantages compared to an angle in the range [0°-360°], that is, a) the existing discontinuity in 360 and 0 degrees is eliminated; b) Hue average of a group of pixels can be understood as the resulting angle of a vector addition of the color pixels in the chromatic region of the sample, giving a simple manner to calculate hue average; c) Setting magnitude to 0 or 1 works as a flag intended for distinction between chromatic or achromatic regions.

2. Separation of chromatic and achromatic regions in the HSI space. We use a separation of the region (according to [2] with possibility of refining with the  $[a_1 \ a_2 \ separation of the region (according to [2] with possibility of refining with the <math>[a_1 \ a_2 \ separation of the region (according to [2] with possibility of refining with the <math>[a_1 \ a_2 \ separation of the region (according to [2] with possibility of refining with the <math>[a_1 \ a_2 \ separation of the region (according to [2] with possibility of refining with the <math>[a_1 \ a_2 \ separation of the region (according to [2] with possibility of refining with the <math>[a_1 \ a_2 \ separation of the region (according to [2] with possibility of refining with the <math>[a_1 \ a_2 \ separation of the region (according to [2] with possibility of refining with the <math>[a_1 \ a_2 \ separation of the region (according to [2] with possibility of refining with the <math>[a_1 \ a_2 \ separation of the region (according to [2] with possibility of refining with the <math>[a_1 \ a_2 \ separation of the region (according to [2] with possibility of refining with the <math>[a_1 \ a_2 \ separation of the region (according to [2] with possibility of refining with the <math>[a_1 \ a_2 \ separation of the region (according to [2] with possibility of refining with the <math>[a_1 \ a_2 \ separation of the region (according to [2] with possibility of refining with the <math>[a_1 \ a_2 \ separation of the region (according to [2] with possibility of refining with the <math>[a_1 \ separation of the region of the region (according to [2] with possibility of refining with the <math>[a_1 \ separation of the region o$ 

# 3.1. Hue Average Calculation

In order to obtain the average of the hue  $(H_m)$  of several pixels from a sample, we take advantage of the vector representation in  $\mathbb{R}^2$ . Vectors that represent the hue values of individual pixels are combined using vector addition. From the resulting vector we obtain two significant values used in the algorithm: average hue and a relative saturation. Thus  $H_m$  is calculated in the following manner:

1. For every pixel P(x,y) in the sample the following  $\mathbb{R}^3$  to  $\mathbb{R}^2$  transformation is applied:

$$V_1(P) = \begin{bmatrix} 1 & -\cos(\pi/3) & -\cos(\pi/3) \\ 0 & \sin(\pi/3) & -\sin(\pi/3) \end{bmatrix} * \begin{bmatrix} R \\ G \\ B \end{bmatrix} = \begin{bmatrix} x \\ y \end{bmatrix}$$
 If  $P \notin G$  (2)

$$V(P) = V_1(P)/|V_1(P)|$$

$$= \begin{bmatrix} 0 \\ 0 \end{bmatrix}$$
If  $P \in G$ 

Where V(P) is the normalized projection of the RGB coordinates of the pixel P to the perpendicular plane to the Intensity axis of the RGB cube when the x axis is collinear to the Red axis of the chromatic circle. On the other hand G (see Section 3.2) represents the achromatic zone in the HSI space and  $[RGB]^t$  is a vector with the color components of the pixel in the RGB color space.

2. Equivalently, the following code is executed:

Vector.x = 0;

Vector.y = 0;

For (i = 1; i < = n; i++)

// for every pixel in the sample do

{Vector.x = Vector.x + V(i).x; // x-component of the accumulated vector Vector.y = Vector.y + V(i).y;} // y-component of the

Vector.y = Vector.y + V(i).y;} // y-component of the accumulated vector

Vs = [Vector.x Vector.y]; // Accumulated vector

In this code we have a vector in R2, which accumulates the vector additions as index i increments. Each of the vectors being added corresponds to the previous  $\mathbb{R}^3$  to

 $\mathbf{R}^2$  transformation for every pixel in the sample made in step 1.

3. The angle of the accumulated vector ( $V_s$ ) with respect to the X-axis is the average hue:

 $H_m$  =angle  $(V_s, 0)$ .

# 3.2. Achromatic Zone G

The achromatic zone G is the region in the HSI color space where no hue is perceived by humans. This means that color is perceived only as a gray level because the color saturation is very low or intensity is either too low or too high.

Given the three-dimensional HSI color space, we define the achromatic zone G as the union of the points inside the cylinder defined by Saturation < threshold\_1 and the two cones Intensity < threshold 2 and Intensity > threshold 3. Pixels inside this region are perceived as gray levels (Fig. 1).

# 3.3. Hue Distance □h

Using the vector representation of Hue obtained by the R3 to R2 transformation of RGB space points expressed in Eq. 2, we can calculate the hue distance,  $\Delta_h$ , between two colors pixels or color centroids  $C_1$  and  $C_2$ , as follows:

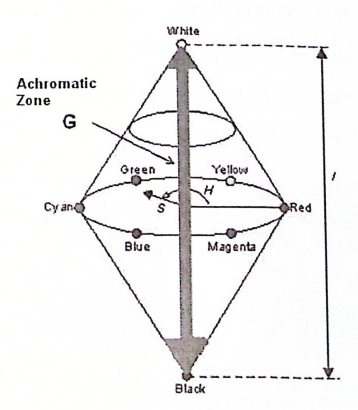


Fig. 1. Achromatic zone G

Where:

abs () = absolute value

dot\_product () = vector dot product

K is a normalizing real factor to force  $\Delta_h \in [0,1]$ 

G is the achromatic region

 $V_1$  y  $V_2$  are the vectors in  $\mathbb{R}^2$  calculated with the transformation on  $C_1$  and  $C_2$  given in Eq. 2.

# 3.4. Saturation Distance and Intensity Distance

Using standard conversions for saturation and intensity from RGB space [2]:

$$saturation(P) = 1 - \left[ \frac{3}{R+G+B} \min(R,G,B) \right]$$
$$intensity(P) = \frac{1}{3} (R+G+B)$$

We define saturation distance,  $\Delta_s$ , and intensity distance,  $\Delta_i$ , between two pixels

 $\Delta_s$  = abs [saturation (P<sub>1</sub>)-saturation (P<sub>2</sub>)], and

 $\Delta_i$  = abs [intensity (P<sub>1</sub>)-intensity (P<sub>2</sub>)]

Where P, P1 and P2 are color pixels or color centroids in RGB space.

# 3.5. Statistical Values for Groups of Pixels

The statistical values needed in Eq. 1 are calculated as follows:

Saturation\_average = 
$$S_c = \frac{1}{n} \sum_{i=1}^{n} saturation(i) * \frac{lenght(vector\_sum)}{\sum_{i=1}^{n} lenght(vector(i))}$$

$$Intensity\_average = I_c = \frac{\sum\limits_{i=0}^{n} intensity(i)}{n}$$
 
$$Hue\_standard\_deviation = \sigma_h = \sqrt{\frac{\sum\limits_{i=1}^{n} \Delta^2_h(i)}{n-1}}$$

$$Saturation\_standard\_deviation = \sigma_s = \sqrt{\frac{\sum_{i=1}^{n} \Delta^2_s(i)}{n-1}}$$

$$Intensity\_standard\_deviation = \sigma_i = \sqrt{\frac{\sum\limits_{i=1}^{n} \Delta^2_i(i)}{n-1}}$$

#### Where

- n is the number of pixels in the sample.
- $\Delta_h(i)$  = hue distance  $\Delta_h(hue(i), hue_average)$ .
- $\Delta_s(i) = \text{saturation\_distance\_}\Delta_s(\text{saturation}(i), \text{saturation\_average}).$
- $\Delta_i$  (i)= intensity\_distance\_ $\Delta_i$  (intensity (i), intensity\_average).

## 3.6. Use of Mathematical Morphology on CSI Images

The CSI image is a gray level image, so it can be dealt with any mathematic morphology technique used for gray level images. Filters, operators, thresholds, etc. can be applied directly to the CSI when geometrical characteristics are considered. The common intensity image can be processed too as a complementary information source.

# **Experimental Results**

In this section we present the results of applying our method to two different color images: a topographic map and an astronomic photography, to perform a comparison with two different published methods: one of scattering type and one that process each pixel as a unit.

Our segmentation method was applied to a section of a topographic map (Fig. 2a). The thematic layers contained in this topographic image are: 1. River layer represented by blue lines; 2. Gross brown elevation isolines; 3. Thin light brown elevation isolines; 4. Extended green area; 5. Green spots.

The procedure is summarized in the following four steps:

1. To segment the river layer, for example, we chose some pixel samples, which looks representative at a simple view as a river (Fig. 2b).





Fig. 2. a) Section of a topographic map; b) Samples obtained from some blue pixels of the river layer

2. Using this 11-pixels sample we calculated the color centroid and the standard deviation:

Color centroid {H<sub>c</sub> 
$$\in$$
 [0, 2 $\pi$ ]; S<sub>c</sub>  $\in$  [0, 1]; I<sub>c</sub>  $\in$  [0, 255]} = (3.56, 0.4126, 102)  $\sigma_{ti} = 0.0392$ ;  $\sigma_{si} = 0.0884$ ;  $\sigma_{ti} = 0.0382$ 

3. Then we generated the corresponding CSI of the sample image (Fig. 3).

4. We applied a simple threshold in this image to segment the river layer (Fig 4). The range of threshold values is very wide (similar results were obtained in the range between 10 and 150); finally, we choose the threshold value equal to 30.

We observed that even with a coarse selection of the pixel sample, we obtained a good separation of this layer. Several different pixel samples were taken when the number of pixels varies from 3 to 11; all of them gave very good results.

Looking at the sample image (Fig. 2) we can observe that color is a fundamental characteristic to discriminate the river layer. That means no other layer has a color, which a human could confuse with that of the river layer. You can see that the blue text *Real* in the original image was segmented also without any problem because it is also represented with blue pixels. That is why we can segment it so easily only with any one of the wide range of threshold possible values applied to the corresponding CSI. This does not happen with other layers in this image; thus, additional morphologic processing could be necessary. In some cases previously extracted layers are necessary to extract some others (case of Fig. 14).



Fig. 3. CSI of blue pixels



Fig. 4. Thresholding with value 30 the CSI shown in Fig. 3

Similarly, we operated in the same way over the remaining layers with linear topographic objects having different colors. Figure 5 shows the pixel samples from the
gross brown isolines layer used to obtain its correspondent CSI shown in Fig. 6. Figure 7 shows the thresholding of the obtained CSI with a value of 80. It can be considered very acceptable as input for recognition, but we can refine it in this way: Applying an opening with a 3x3 square structuring element to eliminate small disconnected
areas (with less of 20 pixels). Figure 8 shows the resulting image.



Fig. 5. Samples obtained from the gross brown isolines



Fig. 6. CSI of the selected brown tone



Fig. 7. Thresholding of the CSI image with threshold 80



Fig. 8. Segmentation of gross brown isolines



Fig. 9. CSI image of thin light brown isolines

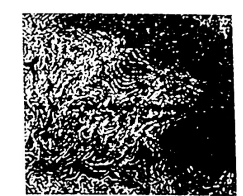


Fig. 10. Thresholding the image in Fig. 9 with threshold 150



Fig. 11. Segmentation of thin green light brown isolines



Fig. 12. Segmentation of green area



Fig. 13. Segmentation of spots

To improve the quality of Fig. 10 we subtract the dilation (done with a 3x3 square structuring element) of Fig 8. The result is shown in Fig 11. In cases of the extended green area and the green spots we present the final results in Fig. 12 and Fig.13, respectively.

Now we process the same map using the software R2V from Able Software Corp [32]. This software performs line recognition additionally to segmentation, thus not all the points shown are obtained from the segmentation step. Results are shown in Figs. 14 to 18.





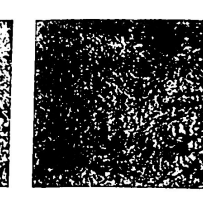


Fig. 14. Segmentation of the river layer

Fig. 15. Segmentation of the gross brown isolines

Fig. 16. Segmentation of the thin light brown isolines

After comparing the results of our solution with those obtained from the software R2V, we can observe that with R2V there are a large number of pixels that should appear in the segmentation of the layer but they do not belong to it. On the other hand, as a worst case, Fig. 14 appears practically empty. We can observe also in results from R2V that the quality of the segmentation is so low, that a considerable number of the pixels appearing in it really belong to other layers. For example, in Fig. 16, in the segmentation of gross brown isolines appear many pixels from the green area that should not be there, and in Fig. 17 appears pixels from all layers.

The second image tested is an astronomic photography in RGB true color shown in Fig. 19 In this case we only process the red zone. The pixel sample selection is shown in Fig. 20 and its corresponding CSI in Fig. 21. The final segmentation can be obtained after thresholding this CSI image. In Fig 22 is shown with a threshold value of 120.



Fig. 17. Segmentation of green area



Fig. 18. Segmentation of green spots



Fig. 19. Testing image for the red zone



Fig. 20. Samples



Fig. 21. CSI image

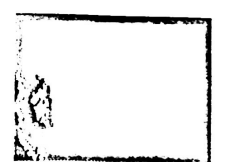


Fig. 22. Thresholding with value 120

Our results are compared with another method which uses color as a unit explained in detail in [1]. The Hue component of Fig 19 is displayed in Fig 23. Figure 24 and Fig. 25 show intermediate processing steps to finally obtain the segmented image shown in Fig. 26.











Fig. 23. Hue component

Fig. 24.

Fig. 25.

Fig. 26. Segmented

As we can visually appreciate, the improvement in quality of our segmentation method is significant. In Fig 21 and Fig. 22 we can easily appreciate that the general form of the red zone is maintained during the process. The final segmentation only requires the thresholding of a CSI with a wide range of values from a raw pixel sample selection.

#### Conclusions 5.

From the analysis of results we can state that the segmentation method presented in this paper offers a useful and efficient alternative for the segmentation of objects in relatively complex color images. We cannot say the same about R2V because none of the results is even close in quality to the thresholded one CSI image obtained by us. This says us a clue that in R2V the segmented information cannot be used efficiently in next stages as those images obtained with the Color Similarity Images created by our method. From experiments in many different maps, not shown here because of a lack of space, we can assess now the advantages of our technique.

The steps required to obtain a good segmentation of objects in the layer of interest are usually straightforward, simple and repetitive. If color is a discriminative characteristic in the layer of interest, only the selection of a given threshold in CSI is needed to obtain a good segmentation result. From many experiments we observed that a good percentage of layers were obtained in a straightforward way only by thresholding the Color Similarity Image.

In our method, the three color components (RGB) of every pixel transformed to the HSI color model are integrated in two steps: in the definitions of distances  $[\Delta_h, \Delta_s,$  $\Delta_i$  in hue, saturation and intensity planes and in the construction of an adaptive color similarity function that combines these three distances assuming normal probability distributions. Thus the complexity is linear with respect to the number of pixels of the source image. Our method discriminate whichever type of different color objects (layers) independently on their shapes in a very straightforward way.

#### Acknowledgments

The authors of this paper wish to thank the Computing Research Center (CIC), Mexico; General Coordination of Postgraduate Studies and Research (CGPI), Mexico, and National Polytechnic Institute (IPN), Mexico, for their support.

#### References

- Gonzalez R.C., Woods R.E. "Digital Image Processing", Prentice Hall Third Edition, USA 2008.
- Plataniotis, K.N., Venetsanopoulos A.N, "Color Image Processing and Applications", 1st Edition Springer Germany 2000, 354pp.
- Alvarado-Cervantes R., Master in Science Thesis, "Segmentación de patrones lineales topológicamente diferentes, mediante agrupamientos en el espacio de color HSI", Center for Computing Research, National Polytechnic Institute, Mexico, 2006.
- Felipe-Riverón, E. M., García-Ramos, M. E. Levachkine S. P., "Problemas potenciales en la digitalización automática de los mapas cartográficos en colores" Proceedings of International Congress on Computation CIC IPN '2000, Mexico City, Mexico 2000.
- Felipe-Riverón, E. M., García-Ramos M. E., "Enhancement of Digital Color Halftoning Printed Images", GEOPRO 2002 ISBN: 970-18-8521-X, México.
- Angulo J., Serra J., "Mathematical Morphology in Color Spaces applied to The Analysis of Cartographic Images", GEOPRO 2003 México.
- Hanbury, A., Serra, J. "A 3D-polar Coordinate Colour Representation Suitable for Image Analysis", Technical Report PRIP-TR-77 Austria 2002.
- Angulo J., Serra J., "Modelling and segmentation of colour images in polar representations", Image and Vision Computing 25 (2007) 475-495 Centre de Morphologie Mathématique - Ecole des Mines de Paris, France.
- Bodansky, E. "System Approach To A Raster-To-Vector Conversion: From Research To Commercial System", GEOPRO 2002 ISBN 970-18-8521-X, México.
- Cheng H., Jiang X, Sun Y., Wang J., "Color image segmentation: Advances and prospects", Pattern Recognition 2001, 34(12), 2259-2281.
- Velázquez A., Levachkine S. P. "Text/Graphics Separation In Raster-Scanned Color Cartographic Maps", GEOPRO 2002, ISBN 970-18-8521-X, México.
- 12. Levachkine S. P., Velázquez A. et a.l., "Color Image Segmentation and Representation Using False Colors", Reporte Técnico #140, Serie Azul, CIC-IPN. México 2002.
- Levachkine S. P., "System Approach to R2V Conversion for Analytical GIS", GEOPRO 2002, Mexico ISBN 970-18-8521-X.
- Levachkine, S. P., Polchkov, E. A., "Cartographic Pattern Recognition", Reporte Técnico #54, Serie: Azul CIC-IPN. México 2000.
- Levachkine, S. P., Alexandrov, V., "Semantic-mind analysis and objected-oriented data integration of visual information: a Primer", GEOPRO 2003-ISBN: 970-36-0111-1, México.
- Levachkine S. P. Velázquez A., Alexandrov V., Kharinov M.," Semantic Analysis and Recognition of Raster-Scanned Color Cartographic Images", GEOPRO CIC IPN México 2002.
- Bourbakis N., Yuan P., Makrogiannis S., "Object Recognition Using Wavelets, L-G graphs and Synthesis of Regions", Pattern Recognition 40 (2007) 2077 – 2096, Elsevier.

- E.L. van den Broek, Schouten Th.E., Kisters P.M.F., "Modeling Human Color Categorization", Pattern Recognition Letters 2007, Elsevier.
   Kim C., You B.J., Jeong M.H., Kim H., "Color Segmentation Robust To Brightness Variations By Using B-Spline Curve Modeling ", Pattern Recognition 41 (2008) 22 37, Electrical Pattern Recognition 41 (2008) 23 37, Electrical Pattern Recognition 41 (2008) 23 37, Electrical Pattern Recognition 41 (2008) 22 37, Electrical Pattern R
- Lim J., Park J., Medioni G.G., "Text Segmentation in Color Images Using Tensor Voting", Image and Vision Computing 25 (2007) 671-685, Elsevier.
- Macaire L., Vandenbroucke N., Postaire J.G., "Color Image Segmentation By Analysis Of Subset Connectedness And Color Homogeneity Properties", Computer Vision and Image Understanding 102 (2006) 105-116, Elsevier.
   Shi L., Funt B., "Quaternion Color Texture Segmentation", Computer Vision and Image Understanding 107 (2007) 88-96, Elsevier.
- 23. R2V, Able Software Corp., http://www.ablesoftware.com